Sensors & Transducers, Vol. 27, Special Issue, May 2014, pp. 221-224

Sensors & Transducers

© 2014 by IFSA Publishing, S. L.
http://www.sensorsportal.com

Sn Doped In_2S_3 Films Elaborated by Spray Technique

[1] M. KRAINI, [1] N. BOUGUILA, [2, 3] A. TIMOUMI, [1] S. ALAYA
[1] Laboratoire de Physique des Matériaux et des Nanomatériaux appliquée à l'Environnement,
Faculté des Sciences de Gabès, Cité Erriadh Manara Zrig 6072 Gabès, Tunisie
[2] Laboratoire de Photovoltaïque et Matériaux Semiconducteurs, Département de Génie Industriel,
Ecole Nationale d'Ingénieurs de Tunis, PB 37, Le Belvédère, 1002, Tunisie
[3] Department of Physics, College of Applied Science, Umm AL-Qura University,
Makka El Mukarrama, Saoudia Arabia, KSA
[1] Tel.: +216 96 490 722, fax: +216 75 392 421
E-mail: mabrouk.karini@gmail.com

Received: 23 November 2013 /Accepted: 12 January 2014 /Published: 26 May 2014

Abstract: Tin doped In_2S_3 films were grown by the chemical spray pyrolysis (CSP) method using the pneumatic spray set-up and compressed air as a carrier gas. The spraying solution contained indium chloride ($InCl_3$), thiourea [$CS(NH_2)_2$] and ($SnCl_4$) at a molar ratio of S/In = 2.5. The deposition was carried out at 350 °C on glass substrates. The Sn doping level was changed with Sn/In = 0-8 % in solution. The effect of Sn concentration on electrical, optical and structural properties of In_2S_3:Sn thin films have been investigated. *Copyright © 2014 IFSA Publishing, S. L.*

Keywords: Indium sulfide, Thin film, Solar cell, Tin doping, Spray pyrolysis.

---

1. Introduction

In_2S_3 is an n type semiconductor exhibiting low conductivity [1] and existing in three crystallographic phases α, β and γ. Among these structures, β-In_2S_3 which is the most stable phase at room temperature crystallizes in a normal spinel structure with a high degree of tetrahedral and octahedral vacancy sites [2–4]. Due to large number of cationic vacancies indium sulfide may be acting as a sink for tin incorporation.

Various methods such as spray pyrolysis [5, 6], ultrasonic dispersion [7], chemical bath deposition (CBD) [8], physical vapor deposition [9], Hydrothermal [1], etc., have been used to prepare In_2S_3. Among these methods, spray pyrolysis is selected in this study because it allows to prepare In_2S_3 in large area thin films at low cost.

Only very few investigation have reported to study the effect of tin doping on In_2S_3 thin films. Becker et al. [10] reported that doping of In_2S_3 films prepared by chemical vapor phase transport (CVT) with Sn decreased the resistivity of films. Mathew et al. [11] reported that doping In_2S_3 by introducing Sn into the spray solution by using $SnCl_4$-$5H_2O$ resulted in widening of optical band gap and also it gave highly photosensitive. In contrast, Mathew et al. also reported that doping of films with Sn by thermal diffusion enhanced considerably the conductivity without affecting any of physical properties [12]. Kilani et al. [12] reported that doping In_2S_3 films prepared by CBD by introducing Sn by using $SnCl_2$-$2H_2O$ resulted in widening of optical band gap. Moreover, a precise study on the properties of doped film is essential to control the doping parameters, which is indispensable for its applications.

In this paper, we depict the effect of Sn doping on the structural, optical, and electrical properties of β-In_2S_3 by adding quantities of Sn to the solution.

2. Experiment

In_2S_3 films were deposited on glass substrates by the spray pyrolysis technique. These In_2S_3 thin films were prepared by spraying an aqueous solution of indium chloride ($InCl_3$) and thiourea ($CS(NH_2)_2$) maintaining a ratio of S:In = 2.5. Tin chloride was used as a source of Sn. Doping percentage of Sn was varied as 0.25 % to 8 %, of indium concentration in the precursor solution. The deposition conditions were optimized in order to obtain reproducible and good quality films. Compressed air was used as the carrier gas at a flow rate of 6 l/min. The nozzle-to-substrate distance was approximately 25 cm, and the spraying time was around 15 min. The substrate temperature was maintained at 350 °C within an accuracy of ± 5 °C. When this temperature was reached, the solution was sprayed. Total volume of the sprayed solution was 100 ml and the flow rate of the solution during spraying was adjusted to be 3 l/min and kept constant throughout the experiment. The thickness of the films is determined by double weight method, using the relation:

$$e = \frac{m}{\rho s}, \qquad (1)$$

where m is the thin film mass, S is the area of the deposited films, and ρ is the density of In_2S_3 material. Using the relation (1), we obtained of the thicknesses about 560 nm for all the samples.

Phase formation of the films was studied by a X-ray diffraction (XRD) system using CuKα radiation (1.5406 Å) of a Bruker D8 Advance diffractometer operating at 40 kV, 40 mA. UV–VIS spectrophotometer (Shimadzu UV 3101 PC) was used to investigate the optical properties. The transmission spectrum was recorded at room temperature with normal incidence in the wavelength range of 200 to 2400 nm. Sheet resistance was examined by a Four-point probe.

3. Structural Characterization

We employed the X-ray diffraction technique to get a first impression of the main crystalline phases and the possible orientation of crystallites in the films prepared at different of dopages concentrations.

Fig. 1 shows the XRD patterns of the indium sulfide thin films deposited by spray pyrolysis on glass for different value of Sn doping quantity. All the peaks in the films correspond to the cubic structure of β-In_2S_3 with diffractions from (400), (440), (222) planes (JCPDS Card -32-0456). A cubic crystal has been obtained with a preferred orientation in the direction (222). Impurity phase of Sn_2S_3 can be detected at 2 %. XRD analysis reveals that the films become almost amorphous when tin exceeds 2 at.%. The films become amorphous when tin exceeds 2 at.%.

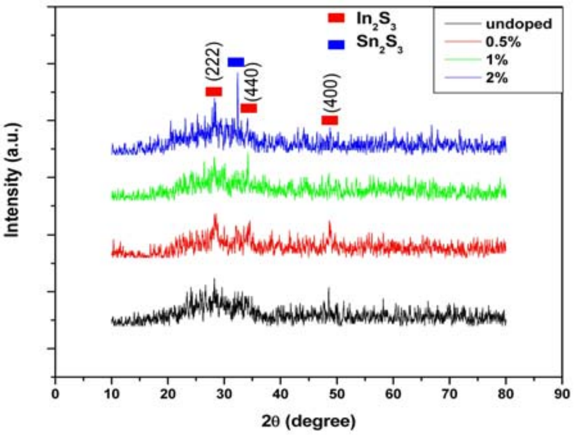

Fig. 1. XRD patterns of In_2S_3:Sn films.

A rough estimate of the grains sizes (D) was made from X-ray diffraction data by using the Scherrer formula [13]:

$$e = \frac{m}{\rho s}, \qquad (2)$$

where Δ(2θ) is the full width at half maximum in radians, λ is the wavelength of X-ray, θ is the Bragg angle.

The evolution of In_2S_3:Sn grain size with tin dopant concentration (Fig. 2). As seen increased grain size with tin deposition.

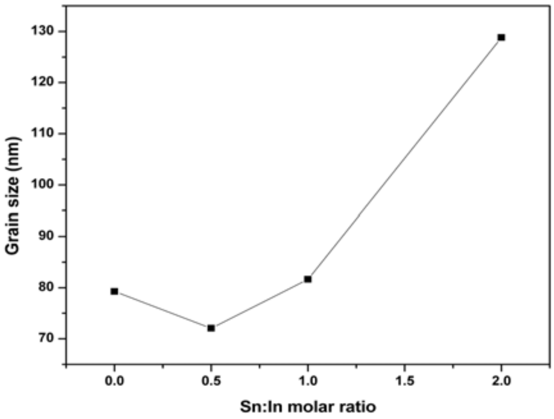

Fig. 2. Grain size variation versus Sn/In ratio.

4. Optical Characterization

Optical transmission measurements in the wavelength range 200–2400 nm is also performed in order to investigate the effect of Sn content on the optical performances of the window layer In_2S_3:Sn.

Fig. 3 shows the optical transmittance of the In_2S_3 films elaborated on glass substrate with different Sn content. All layers show good transmittance reaching 60 % in visible and 80 % in near-IR region.

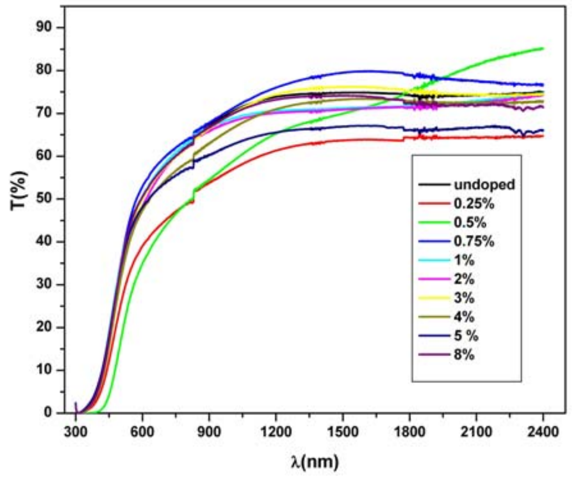

Fig. 3. Transmittance spectra of In_2S_3:Sn films.

The analysis of the dependence of absorption coefficient on photon energy in the high absorption regions is carried out to obtain the detailed information about the band gap energy. The optical band gap of the films is determined by the following relation [14]:

$$\alpha h\nu = A(h\nu - E_g)^n , \qquad (3)$$

where A is the constant, E_g is the optical band gap and the exponent n characterizes the nature of band transition. Indeed, n = 1/2 and 2 corresponds to direct allowed and direct forbidden transitions, respectively. Fig. 4 shows the variation of $(\alpha h\nu)^2$ against hν. The band gap energy is determined by extrapolating the straight line portion to the energy basis at $\alpha = 0$.

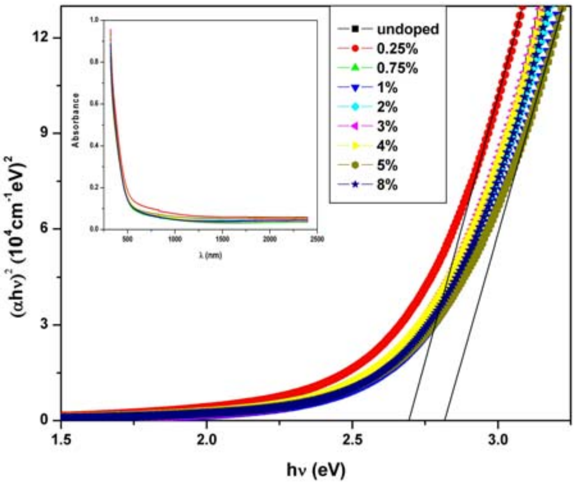

Fig. 4. Plots of $(\alpha h\nu)^2$ vs. (hν) for In_2S_3:Sn thin films, the inset displays the optical absorbance spectra.

We noticed that the gap energy has spent from 2.62 to 2.72 eV. But it is remarkable that this variation is not linear with the dopant concentration. Similar behavior was also observed by Mathew et al. and Kilani et al. [12] who reported that Sn doped In_2S_3 exhibited an increase in band gap with Sn concentration. Presence of Sn in the spray solution enhanced the tendency of oxygen incorporation very much, making the atomic concentration of oxygen in the films greater than that achieved by other techniques. Increase in band gap could be attributed to the contribution of oxygen [11].

The extinction coefficient could be calculated from the equation:

$$k = \frac{\lambda\alpha}{4\pi}, \qquad (4)$$

once the values of absorption coefficient (α) were known. The variation of extinction coefficient with wavelength, for different concentrations of dopage, is given in Fig. 5.

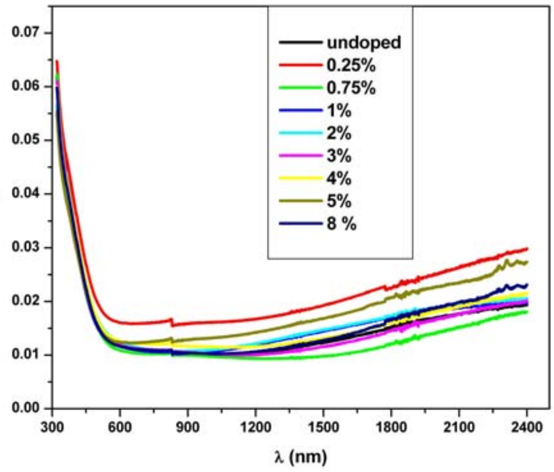

Fig. 5. Extinction coefficient of In_2S_3:Sn films.

5. Electrical Characterization

All the films exhibited n-type conductivity. Resistivity of the as prepared samples was high. In general, the rate of doping giving the best electrical performance depends on the deposition technique, the production temperature and the thickness of the sample.

6. Conclusion

Indium sulfide thin films were elaborated with spray technique for different Sn/In molar ratio. It has been shown that the presence of Sn element may induce important changes in the films properties. The investigation of optical properties revealed that the films exhibited an increase of the band gap with Sn concentration. Depending on the Sn/In ratio, band gap of In_2S_3:Sn could be varied from 2.62 to 2.72 eV. Wide band gap is highly useful for buffer layer applications. Wider band gap will improve light transmission in the blue wavelength.

Acknowledgements

The authors would like to thank Dr J. Ghoul and Dr I. Halidou for helpful discussions. This work is supported by DGRST.

References

[1]. P. G. S. Abadi, M. S. Niasari, F. Davar, Hydrothermal synthesis, characterization and optical properties of 3D flower like indium sulfide nanostructures, *Superlattices and Microstructures*, Vol. 53, 2013, pp. 76–88.

[2]. N. Barreau, Indium sulfide and relatives in the world of photovoltaics, *Solar Energy*, Vol. 83, 2009, pp. 363–371.

[3]. H. Spasevska, C. C. Kitts, C. Ancora, G. Ruani, Optimised In_2S_3 Thin Films Deposited by Spray Pyrolysis, *International Journal of Photoenergy*, Vol. 2012, 2011, pp.1-7.

[4]. C. H. Ho, Y. P. Wang, Y. S. Huang, Optical characterization of band-edge property of In_6S_7 compound, *Applied Physics Letters*, Vol. 100, Issue 13, 2012, pp. 131905-131909.

[5]. T. T. John, M. Mathew, C. S. Kartha, K. P. Vijayakumar, T. Abe, and Y. Kashiwaba, $CuInS_2$/ In_2S_3 thin film solar cell using spray pyrolysis technique having 9.5 % efficiency, *Solar Energy Materials and Solar Cells*, Vol. 89, Issue 1, 2005, pp. 27–36.

[6]. M. Kraini, N. Bouguila, I. Halidou, A. Timoumi, S. Alaya, Properties of In_2O_3 films obtained by thermal oxidation of sprayed In_2S_3, *Materials Science in Semiconductor Processing,* Vol. 16, 2013, pp. 1388–1396.

[7]. Z. Li, X. Tao, Z. Wu, P. Zhang, Z. Zhang, Preparation of In_2S_3 nanoparticle by ultrasonic dispersion and its tribology property, *Ultrason Sonochemistry*, Vol. 16, Issue 2, 2009, pp. 221-225.

[8]. B. Asenjo, C. Sanz, C. Guillén, A. M. Chaparro, M. T. Gutiérrez, J. Herrero, Indium sulfide buffer layers deposited by dry and wet methods , *Thin Solid Films*, Vol. 515, Issue 15, 2007, pp. 6041-6044.

[9]. N. Barreau, J. C. Bernède, C. Deudon, L. Brohan, S. Marsillac, Study of the new β-In_2S_3 containing Na thin films Part I: Synthesis and structural characterization of the material, *Thin Solid Films*, Vol. 241, Issues 1–2, 2002, pp. 4-14.

[10]. R. S. Becker, T. Zheng, J. Elton, M. Saeki, Synthesis and photoelectrochemistry of In_2S_3 , *Solar Energy Mater*, Vol. 13, Issue 2,1986, pp. 97–107.

[11]. M. Mathew, M. Gopinath, C. Sudha Kartha, K. P. Vijayakumar, Y. Kashiwaba, T. Abe, Tin doping in spray pyrolysed indium sulfide thin films for solar cell applications, *Solar Energy*, Vol. 84, 2010, pp. 888–897.

[12]. M. Kilani, C. Guasch, M. Castagne, N. K. Turki, Structural, optical, and electrical properties of In_2S_3:Sn thin films grown by chemical bath deposition on pyrex, *Journal of Materials Science*, Vol. 47, 2012, pp. 3198–3203.

[13]. J. El Ghoul, C. Barthou, L. El Mir, Synthesis by sol–gel process, structural and optical properties of nanoparticles of zinc oxide doped vanadium, *Superlattices and Microstructures*, Vol. 5, 2012, pp. 942–951.

[14]. N. Pentyala, R. K. Guduru, E. M. Shnerpunas, P. S. Mohanty, Synthesis of ultrafine single crystals and nanostructured coatings of indium oxide from solution precursor, *Applied Surface Science*, Vol. 257, 2011, pp. 6850–6857.